# Direct observation of tilted vortex structures induced by twin boundaries in $YBa_2Cu_3O_y$ single crystals

A. A. Zhukov
*Centre for High Temperature Superconductivity, Blackett Laboratory, Imperial College, London SW7 2BZ, United Kingdom and Physics Department, Moscow State University, Moscow 117234, Russia*

G. K. Perkins, J. V. Thomas, and A. D. Caplin
*Centre for High Temperature Superconductivity, Blackett Laboratory, Imperial College, London SW7 2BZ, United Kingdom*

H. Küpfer and T. Wolf
*Forschungszentrum Karlsruhe, Institut für Technische Physik, D-76021 Karlsruhe, Germany*
(Received 2 April 1997)

In twinned $YBa_2Cu_3O_y$ single crystals we have observed that as the magnetic field **H** is tilted away from the $c$ axis, a nearly *reversible* $ab$-plane magnetic moment $m_{ab}$ is generated that has a sharp maximum as a function of the tilt angle $\varphi$; this moment is absent from detwinned samples. Thus the measured direction of the vortices deviates from that of the applied field, reflecting their attraction to the twin boundaries (TB's). For a crystal with a single dominant direction of TB's, the size of $m_{ab}$ at low fields is consistent with ideal shielding of the $ab$-plane field component $H_{ab}$, as expected for the vortex state that is fully locked to the TB's. The maximum in $m_{ab}$ at a fixed temperature occurs at a value of $H_{ab}$ that is nearly independent of $\varphi$; we identify this as the locking field $H_L$. The trapping angle $\varphi_T$, above which the kinked-vortex state vanishes, is apparent in the data too. The qualitative features of these results agree with current understanding of the vortex-TB interaction, but there are several quantitative discrepancies. [S0163-1829(97)06130-4]

## I. INTRODUCTION

The interaction of vortices with twin boundaries (TB's) in $YBa_2Cu_3O_y$ single crystals has been of considerable interest for several years (e.g., Ref. 1–9). The presence of TB's leads to increased pinning at high temperatures,[3–6,8,9] but they can become channels for easier flux penetration at lower temperatures.[2,7–9] Previous studies were based on the comparison of crystals of different twin structures[4,7] or on analysis of the detailed angular dependence of the transport properties.[5–9] Those experiments give information about the influence of TB's on the critical current or on vortex motion, but do not determine directly the vortex orientation with respect to the TB's within the crystal. However, an understanding of the transformations of the vortex structure as the magnetic field is tilted away from the TB's requires precise knowledge of this orientation.

Vortex interaction with TB's was considered theoretically in Refs. 10–12. The appearance of distinct phases was predicted, with the vortex direction becoming noncollinear with the applied magnetic field **H** when **H** is tilted away from the TB plane; we denote this tilt angle as $\varphi$. Theory predicts that when $\varphi$ is less than a critical locking angle $\varphi_L$, vortices are locked to the TB's, so that as **H** is tilted out of the TB plane (rotating from the crystalline $c$ axis toward the $ab$ plane), **B** remains aligned in the TB plane [Fig. 1(a)]. Consequently, in the locked vortex state, the transverse component of the magnetization $M_{ab}$ is equal to $-H\sin\varphi$, so that the $ab$-plane component $H_{ab}$ of the applied field is shielded completely. This ideal shielding of $H_{ab}$ is the distinctive signature of the locked phase.

At large angles $\varphi_L<\varphi<\varphi_T$ [Fig. 1(b)], a kinked vortex structure develops. The tilted vortex segments make an angle $\varphi_T$ with the TB's and link segments that remain locked to the

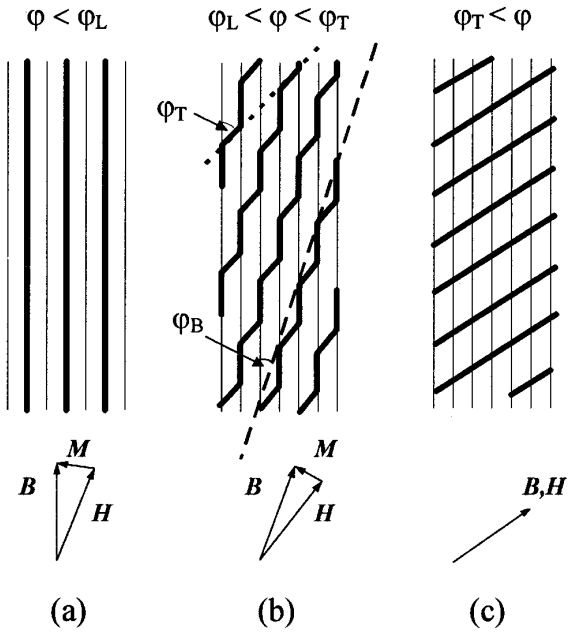


FIG. 1. Transformations in the vortex (thick lines) structure induced by rotation of the applied magnetic field **H** away from the TB's (thin lines): (a) locked, (b) kinked, and (c) collinear vortex phases. The trapping angle $\varphi_T$ is that of the linking vortex segments within the kinked phase; $\varphi_B$ describes the mean vortex direction. The difference in magnitudes of **B** and $\mu_0$**H** is neglected in these schematic diagrams.

 

TB plane. With increasing angle $\varphi$, the length of the locked segments decreases and vanishes when $\varphi=\varphi_T$. Equivalently, the angle between **B** and **H** diminishes and vanishes at $\varphi_T$; therefore, $M_{ab}$ should decrease in this range. The size of $\varphi_T$ is determined by the vortex line tension, so that it is the analog of the liquid meniscus contact angle. The line tension equals the energy $\varepsilon$ per unit length of vortex; balance of the line tensions in the twin plane for the free ($\varepsilon_0$) and trapped ($\varepsilon_T$) segments of the vortex line at their point of connection requires that $\cos\varphi_T=\varepsilon_T/\varepsilon_0$.

Finally, at large angles $\varphi>\varphi_T$ [Fig. 1(c)], the TB's cease to influence the vortex structure, so that $M_{ab}$ falls to the (small) thermodynamic magnetization.

The theory describes the extent of the locked state in terms of a locking field $H_L$, transverse to the TB's and equal to $H\sin\varphi_L$; it yields the expression $H_L=H_{c1}\sin\varphi_T$.[11,12] This result has a straightforward physical interpretation: When the mean direction of a vortex [shown by the dashed line in Fig. 1(b)] tilts by an angle $\varphi_B$ from the TB's, the energy of the vortex system changes from $NL\varepsilon_T$ ($N$ is the number of vortices in the sample) to $E(\varphi)=NL\varepsilon_0\cos(\varphi_T-\varphi_B)$, as can be shown by elementary but tedious calculations. The restoring torque $G_R$ which opposes the rotation of the vortices is given by $-\partial E/\partial\varphi_B$ and, for small angles $\varphi_B$, has constant value $\approx NL\varepsilon_0\sin\varphi_T$. The magnetic driving torque $G_M$ caused by misalignment between **H** and **B** increases with the angle $\varphi$ between **H** and the TB's: $G_M=\mu_0|\mathbf{m}\times\mathbf{H}|=\Omega|\mathbf{B}\times\mathbf{H}|\approx NL\phi_0 H\sin(\varphi-\varphi_B)$, where $\Omega$ is the sample volume; vortex rotation starts when the critical locking angle $\varphi_L=\arcsin[\varepsilon_0\sin\varphi_T/(\phi_0 H)]$ is exceeded. Taking into account that for small $\varphi_T$ and low vortex density, $\varepsilon_0/\phi_0=H_{c1}[\ln(a_0/\xi)/\ln(\lambda/\xi)]$, the expression for the corresponding locking field $H_L\approx H_{c1}\sin\varphi_T$ follows.

## II. EXPERIMENT

With the scenario described above in mind, we carried out magnetic studies of several $YBa_2Cu_3O_y$ single crystals grown from the flux,[13] with the aim of looking for direct evidence of these theoretically predicted phases. The crystals studied had a variety of twin structures and varied in concentration of pointlike defects. Two of these samples (MK and WZ) were detwinned,[8] and two others were densely twinned. One of the latter (AM) had both directions of TB's, but the other (OZ) was cut from a larger crystal and, as viewed in a polarized light microscope, had TB's of predominantly one direction. The present study focuses on the behavior of this last crystal of dimensions $1.95\times1.15\times0.065$ mm$^3$, with the long side parallel to the TB's; its $T_c$ is 91.3 K. Transmission electron microscopy of a crystal from the same batch showed typical TB spacing of $\sim$100 nm.[9]

A vibrating sample magnetometer (Oxford Instruments $5^H$) was used for these studies; it is equipped with two independent coil sets that measure simultaneously the magnetic moments parallel (standard component $m_{\rm std}$) and perpendicular (ortho component $m_{\rm ort}$) to **H** (Fig. 2). The sample can be rotated *in situ* about the third axis, with an angular resolution of 0.01° and reproducibility better than 0.1°. Great care was taken to avoid misalignment and misorientation artifacts.[14] Magnetization loops up to 5 T were taken at a sweep rate of 14 mT s$^{-1}$ and at fixed angle, because the converse protocol of sample rotation at fixed field can induce deviations from the critical state.

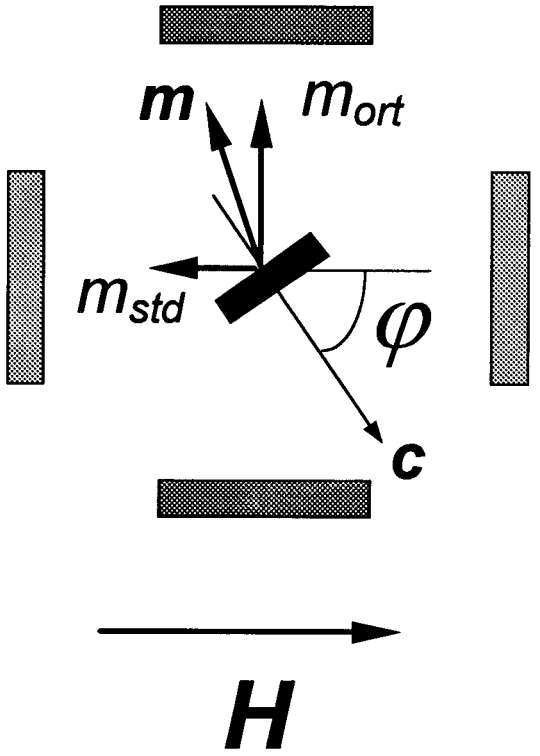


FIG. 2. Experimental configuration for measurement of the vector magnetic moment; the shaded regions represent the two sets of coils that monitor simultaneously the moments parallel ($m_{\rm std}$) and perpendicular ($m_{\rm ort}$) to the applied field.

Conventional (single-channel) magnetometers[4,7,8] measure only the $m_{\rm std}$ component of **m**; with torque magnetometers,[6] the signal is proportional to $m_{\rm ort}$; hence, neither instrument can provide full information about **m**. Direct visualization of the magnetic flux[2,3] or of the vortices[1] gives a picture of the normal component of the magnetic induction at the sample surface, but no information about the interior. The advantage of our approach is its ability to measure both magnetic moment components and so to determine the components along the principal crystallographic directions $m_{ab}=m_{\rm std}\sin\varphi+m_{\rm ort}\cos\varphi$ and $m_c=m_{\rm std}\cos\varphi-m_{\rm ort}\sin\varphi$; it is therefore a *direct* method for study of the tilted vortex phases.

The angle $\varphi_B$ between the average vortex direction and the TB plane is given by $\tan\varphi_B=B_{ab}/B_c$, where the transverse component is that in the direction perpendicular to the TB's. Demagnetizing factors often complicate the relationship between **B**, **H**, and **M** in HTS crystals, which are nearly always thin plates. For $M_{ab}$, demagnetization is negligible, so that $B_{ab}=\mu_0(H_{ab}+M_{ab})$. For the field component parallel to the $c$ axis, we concentrate on the regime of large fields, with $H_c$ greater than the demagnetizing self-field $H_S$. Then we may put $B_c\approx\mu_0 H_c$ and finally express $\varphi_B$ in terms of directly measured quantities as

$$\tan\varphi_B\approx\left(\tan\varphi+\frac{m_{ab}}{\mu_0 H_c\Omega}\right). \tag{1}$$

Even though Eq. (1) is not exact (because of demagnetiz-

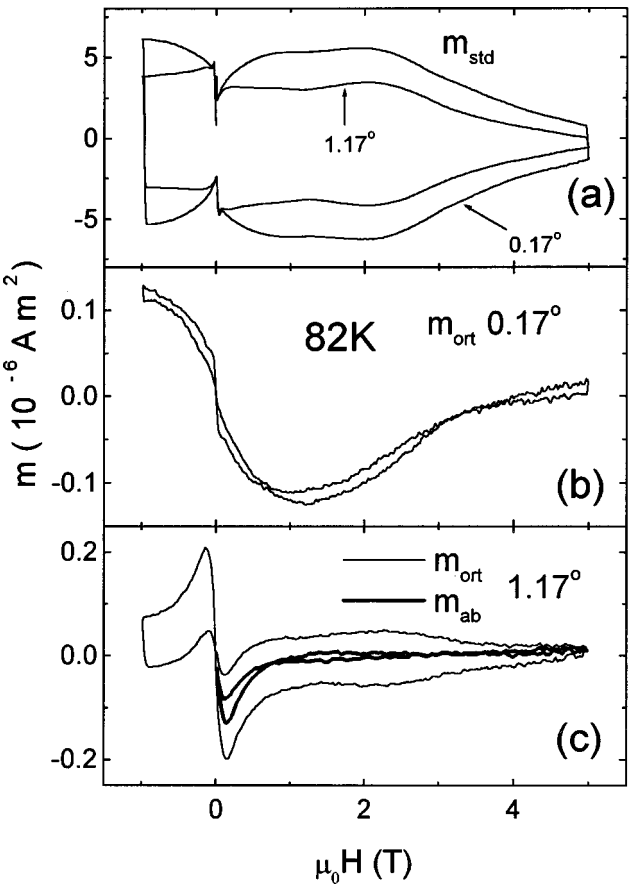


FIG. 3. Magnetic field dependences of the magnetic moment at 82 K of the twinned crystal OZ for two small angles between **H** and the TB plane: (a) the moment $m_{\rm std}$ parallel to **H**, (b) the moment $m_{\rm ort}$ perpendicular to **H**, and (c) $m_{\rm ort}$ compared with the moment $m_{ab}$ in the $ab$ plane of the crystal. The penetration field for $\mathbf{H}\|c$ is ~20 mT.

ing effects), for small angles $\varphi$ the variations of $\varphi_B$ are well described by the changes of $m_{ab}$; that is, $m_{ab}/H_c$ is proportional to the angle $(\varphi\text{-}\varphi_B)$ between **B** and **H**.

## III. RESULTS AND DISCUSSION

For a direct check of the theories,[10–12] we use the data taken at high temperatures ($\geqslant$60 K), where TB pinning is dominant[8] and self-field effects are small, so that we can easily attain the condition $H>H_S$. At lower temperatures there is significant vortex channeling and the vortex state becomes inhomogeneous.

### A. Reversible and irreversible moments

Neglecting self-fields, the magnetization resulting from **B** and **H** noncollinearity in the locked and kinked vortex phases should be essentially reversible (cf. Fig. 1). The reason is that the line tensions that determine the equilibrium (nonhysteretic) configurations shown in Fig. 1 are of the order of the large transverse (to the TB) pinning force, whereas the hysteretic Lorentz force (it has opposite sign for increasing and decreasing magnetic fields) is equal to the much smaller longitudinal TB pinning force.

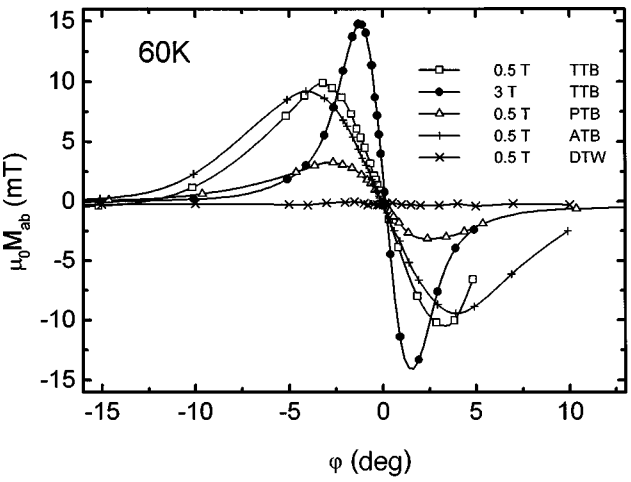


FIG. 4. Reversible magnetization $M_{ab}$ of the OZ crystal at 60 K as the magnetic field is rotated away from the $c$ axis ($\varphi=0$). The different curves correspond to the rotation plane being perpendicular (TTB), parallel (PTB), and at ~45° (ATB) to the dominant TB planes. For comparison, the behavior of the detwinned MK crystal (DTW) is shown too. Here and in the later figures, the lines are guides to the eye.

A second crucial feature of our experimental configuration is that *irreversible* screening currents give negligible contribution to $m_{ab}$, whereas they nearly always dominate $m_c$. The reason for this lies in the platelike geometry of the crystals and is independent of the details of their superconducting behavior.[15,16] Quite generally, the critical state set up in a superconducting plate has its (irreversible) magnetic moment **m** closely parallel to the plate normal **n** (in our case the crystalline $c$ axis), even when the applied field **H** is at large angles to **n**. Only when **H** is nearly parallel to the plane, within an angle $\sim t/w$ where $t$ is the plate thickness and $w$ its width, is there a significant irreversible moment in the transverse direction; the present experiments never enter that regime. Hence this geometrical effect assists the observation of the reversible transverse moment $m_{ab}$ associated with the noncollinear vortex phases induced by interaction with the TB's.

### B. Angular dependence of *m*

Both the twinned crystals show strong angular dependences of $m_{\rm std}$ and $m_{\rm ort}$ as **H** is tilted away from the $c$ axis; sample OZ (Fig. 3) was oriented so that the rotation plane was perpendicular to the plane of the majority TB's. Note that at these small angles, $m_{\rm std}$ is dominated by its hysteretic component, whereas for $m_{\rm ort}$ the reversible contribution is the larger. Moreover, the resolved component $m_{ab}$ in the direction perpendicular to the TB's shows very small irreversibility over most of the angular range [e.g., Fig. 3(c)], as anticipated in the previous section.

Because the irreversibility of $m_{ab}$ is small, from here on we consider only its reversible component, as obtained from the average of upward and downward legs of the **m-H** loops. For a given field, both twinned crystals show maxima in $m_{ab}$ as a function of $\varphi$ (Fig. 4). At larger fields this peak becomes sharper and shifts closer to the $c$ axis. At somewhat higher angles $m_{ab}$ becomes small, and thereafter hardly changes until the direction of **H** approaches the $ab$ plane.

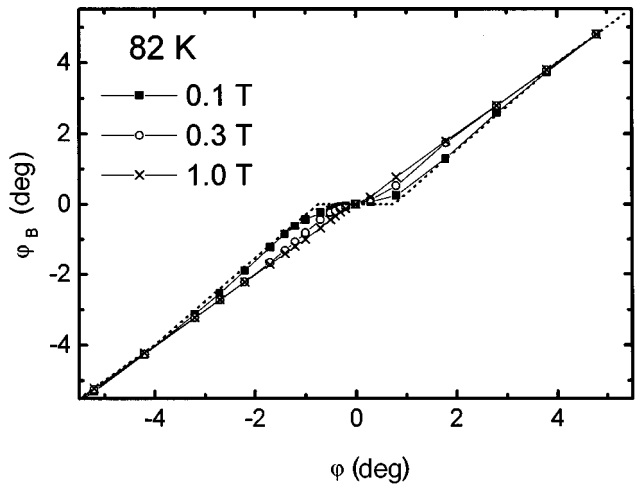


FIG. 5. Dependence of the vortex direction $\varphi_B$ on field direction $\varphi$ in the OZ crystal at 82 K, as **H** is rotated away from the $c$ axis in the plane perpendicular to the dominant TB planes. The dashed line is the theoretical dependence (Ref. 11) for $\varphi_L = 0.75°$ and $\varphi_T = 4°$.

Several features prove that this behavior of $m_{ab}$ in crystal OZ is associated with the TB's in that sample: First and foremost, both detwinned crystals have vanishingly small $m_{ab}$ (Fig. 4). In a second experiment the OZ crystal was remounted so that the rotation plane of **H** lay parallel to the plane of the majority TB's. In this configuration, $m_{ab}$ has a similar angular dependence to that when **H** is tilted perpendicular to the plane of the dominant TB's, but is smaller by a factor ~3, that is, nearly field and temperature independent. This result suggests that in fact ~25% of the TB's in the OZ crystal are orthogonal to the dominant orientation, even though optical microscopy showed only traces of them; presumably, they are present on a submicrometer scale. In a final experiment on crystal OZ, it was mounted so that the rotation plane of **H** lay at an angle of about 45° with the TB plane. Now $m_{ab}$ diminishes as compared with the first experiment, and the angle of the maximum increases, as would be expected from simple geometrical considerations based on the projection of **H** normal to the TB's.

We use Eq. (1) to determine the (mean) vortex direction $\varphi_B$. In our experimental regime, the angular window in which $\varphi_B$ deviates from $\varphi$, the angle of the applied field, is very narrow (Fig. 5). As **H** is rotated away from the $c$ axis, $\varphi_B$ at first increases very slowly, with a plateau that is more marked at low applied fields. Here the vortices prefer to orientate parallel to the TB planes and so deviate from the applied field direction. At large angles, the vortex direction asymptotically approaches that of **H**, in reasonable accord with theory[11] (shown by the dashed line in Fig. 5):

$$\varphi_B = 0 \quad \text{for} \quad \varphi < \varphi_L,$$

$$\varphi_B = \varphi_T(\varphi_T - \varphi) \quad \text{for} \quad \varphi_L < \varphi < \varphi_T, \tag{2}$$

$$\varphi_B = \varphi \quad \text{for} \quad \varphi_T < \varphi.$$

In a simple picture of the locked state, $\varphi_B$ would be identically zero. However, in practice there are several possible reasons for a finite value: (i) the presence of TB's with another direction, (ii) penetration of vortices into the crystal in regions of low TB density, and (iii) thermally activated vortex tilt, which should become particularly important as $\varphi$ approaches $\varphi_L$, where the energy difference between locked and kinked states vanishes.

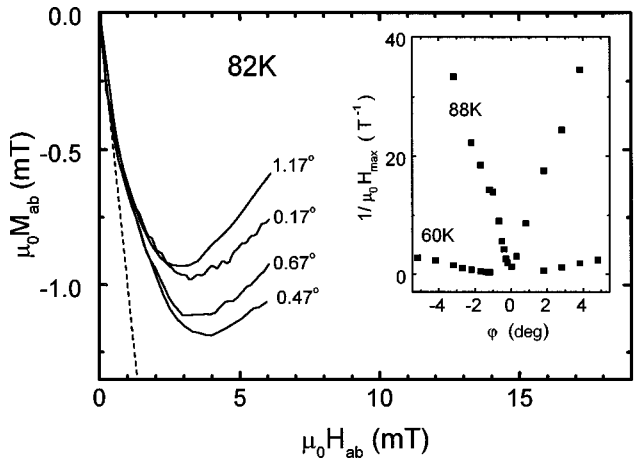


FIG. 6. The dependence of the $ab$-plane magnetization $M_{ab}$ on the $ab$-plane magnetic field component $H_{ab}$ at 82 K; the dashed line has slope $-1$. The inset shows the angular dependence of the peak value $H_{\max}^{-1}$ for the rotation plane of **H** perpendicular to the majority TB plane, as obtained from $m$-$H$ loops such as Fig. 3(c).

### C. Shielding of the transverse field

Figures 6 and 7 show a quantitative test of the perfect shielding of the in-plane field component ($H_{ab}$) that is a signature of the locked vortex state. When plotted against $H_{ab}$, the initial slope of the in-plane magnetization $M_{ab}$ of crystal OZ is indeed close to $-1$ (note again that demagnetizing effects are insignificant for this direction). Since this magnetic response is observed to be reversible, we refer to it as the transverse Meissner effect.

At higher fields, the slope $dM_{ab}/dH_{ab}$ continuously decreases in magnitude and $M_{ab}$ drops well below the full-shielding value. Even within a locked vortex state, the fac-

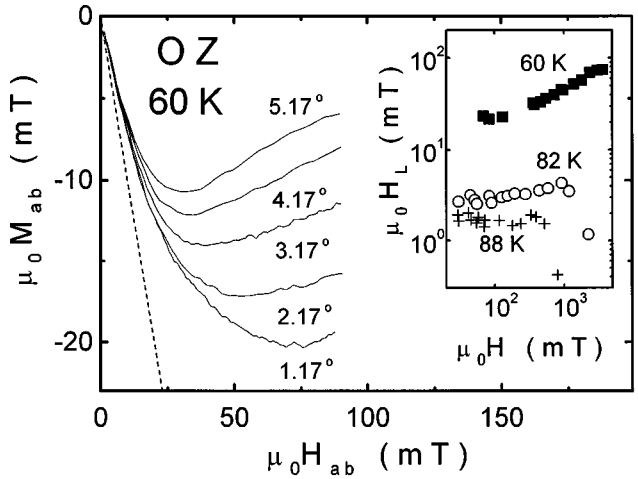


FIG. 7. Dependence of the $ab$-plane magnetization $M_{ab}$ on the $ab$-plane magnetic field component $H_{ab}$ at 60 K; the dashed line has slope $-1$. Inset: dependence of the locking field $H_L = H \sin \varphi_L$ on applied field $H$ at 60, 82, and 88 K.

tors previously mentioned can suppress the shielding: (i) the presence of TB's with another direction, (ii) penetration of vortices in regions of low TB density, and (iii) thermally activated vortex tilt. Consequently, it is not surprising to observe a continuous and gradual reduction in $(dM_{ab}/dH_{ab})$, rather than a discontinuity that would signal a sharp transition from locked to kinked states.

We stress that in our experiments we observe the shielding of the transverse field component with the crystal at a *fixed* orientation. In experiments in which the sample is rotated in the magnetic field, screening currents and irreversible magnetic moments are induced that can easily confuse the situation. Several previous studies (e.g., Ref. 17) have reported observation of the vortex-locked state induced by the CuO planes; however, this interpretation was based on torque measurements obtained during sample rotation. Indeed, we have demonstrated that when a thin plate of a *conventional* superconductor ($V_3Si$) is rotated so that its plane swings away from the direction of **H**, a transverse moment is induced that corresponds to perfect shielding.[18] Thus, in a rotation experiment, the electromagnetic response is that of the induced screening currents and the transverse magnetization is strongly irreversible.

By working at fixed sample orientation, we avoid these problems. As the data for the untwinned crystal show (Fig. 4), in the absence of TB's, the transverse magnetization is zero and there is no transverse shielding. Conversely, the reversible transverse shielding observed in the twinned sample is unambiguously associated with the presence of the TB's and does not arise from electromagnetic induction artifacts.

### D. Locking angle

Theory[10,11] predicts maximum misalignment between **B** and **H** at the transition from locked to kinked states and that this transition is determined by the magnitude of $H_{ab}$ alone. It is therefore reasonable to associate the peak of $M_{ab}$ with this transition. We may also identify the corresponding value of $H_{ab}=H_{\max}\sin\varphi\approx H_{\max}\varphi$ as the lock-in field $H_L$. The field position $H_{\max}$ of the observed peak in $m_{ab}$ (or $M_{ab}$), as seen in the data of Fig. 4, does indeed follow an approximate inverse dependence on $\varphi$ at low fields (inset to Fig. 6). However, at low temperatures, the dependence is better described by $H_{\max}^{-1}=\varphi H_{L0}^{-1}-H_0^{-1}$, which differs from the expression for a constant $H_L$ by the term $H_0^{-1}$. The value of $\mu_0 H_{L0}$ determined from the linear slope of $H_{\max}^{-1}(\varphi)$ increases rapidly with temperature from 1.7 mT at 88 K to 25 mT at 60 K. The parameter $\mu_0 H_0$ is 1.6 T at 60 K.

The observed increase of $H_L=H_{\max}\sin\varphi$ at higher fields (inset to Fig. 7) and also the subsequent decrease near the irreversibility field may be connected with the influence of collective interactions.[12] Deviations from constancy may be expected when the applied field exceeds the matching field of the twin structure, which for our crystals we estimate to be about $10^{-1}$ T; this criterion agrees rather well with the observed behavior.

### E. Irreversible magnetization and the trapping angle

The influence of the TB's on the shielding currents of density $j_s$ (measured by the *irreversible* part of the magnetic moment $\Delta m_c$) that circulate in the $ab$ plane is shown in Fig. 8; to take account of the intrinsic angular dependence of the parameters, the data are plotted at fixed $c$ component of the field $H_c=H\cos\varphi$.[11,16,19] The detwinned MK sample with dominant pointlike disorder pinning has $j_s$ independent of $\varphi$ up to $\sim 60°$. In contrast, the OZ crystal exhibits a very strong angular dependence, but with a somewhat blunt peak within the locking-angle range (note that, for the same reasons as may account for the deviation from ideal shielding of $H_{ab}$, $j_s$ is not angle independent in that range). For $\varphi>\varphi_L$, there is a rapid drop in $j_s$ and it vanishes at large angles.

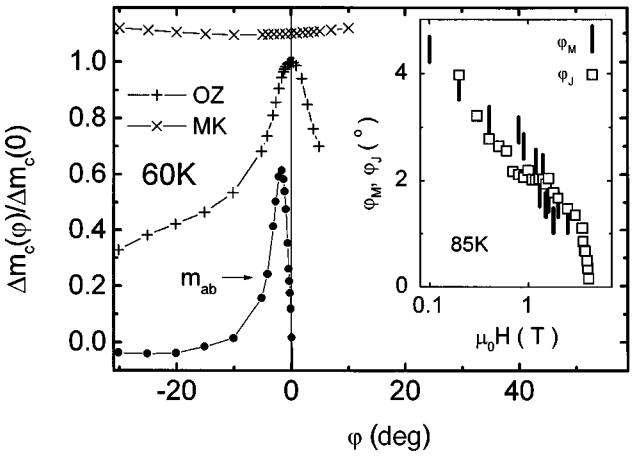


FIG. 8. Relative angular dependences of the irreversible magnetic moment $\Delta m_c$ for the OZ (twinned) and MK (detwinned) crystals at 60 K at constant $\mu_0 H_c$ $(=\mu_0 H\cos\varphi)$ of 1.5 T; for clarity, the latter data are displaced upward by 0.1 units. For comparison of the angular dependences, the reversible $m_{ab}$ of crystal OZ is included too (arbitrary units). Inset: dependence of the characteristic angles $\varphi_J$ and $\varphi_M$ (see text) on field at 85 K, where the irreversibility field of $\sim 4$ T is within the experimental window.

As Fig. 8 shows, the angular width of the peak in the *irreversible* screening currents $j_s$ associated with the vortex-TB interaction is comparable to the width of the peak in the transverse *reversible* moment $m_{ab}$. We therefore identify this angle as the boundary of the kinked state, which is the trapping angle $\varphi_T$; again, the transition is likely to be smeared, because of thermal and other factors.

In the kinked vortex state, a linear dependence of $j_s$ on $\varphi$ may be expected: If bulk pinning can be neglected,[8] the pinning force is that acting on the locked segments of vortex line [Fig. 1(b)], so that $F=f_{\rm TB}L(1-\tan\varphi_B/\tan\varphi_T)$, where $f_{\rm TB}$ is the pinning force to the TB's in a direction parallel to the TB plane per unit vortex length (the dissipation is determined by vortex motion along the TB planes, induced by currents transverse to the TB's), $\varphi_B$ defines the average direction of **B** [Fig. 1(b)], and $L$ is the crystal thickness. On the other hand, for fixed $j$ and $|\mathbf{B}|$, the Lorentz force component parallel to the $ab$ plane does not change with $\varphi_B$. Therefore the angular dependence $j_c(\varphi)=j_c(0)(1-\tan\varphi_B/\tan\varphi_T)\approx j_c(0)(1-\varphi/\varphi_T)$ is expected [we have used the relation[11] $\varphi_B=\varphi_T(\varphi-\varphi_L)/(\varphi_T-\varphi_L)\approx\varphi$, valid for $\varphi_T\gg\varphi_L$].

As the inset to Fig. 8 shows, the angle $\varphi_J$ at which $j_s(\varphi)$ drops most steeply is in good agreement with the angle $\varphi_M$, the angle at which $m_{ab}$ has dropped to $\sim 5\%$ of its peak value (an arbitrary criterion, but one chosen to represent the

last vestiges of the influence of the TB's on the vortex direction), so that we may regard them both as good measures of the trapping angle $\varphi_T$. The data shows initial near-logarithmic variations of $\varphi_J$ and $\varphi_M$ with field, which agrees with the theoretical variation of $\varphi_T$,[12] but then decrease more rapidly as the irreversibility field is approached. For $\mu_0 H = 1$ T, we estimate $\varphi_T$ to be $\approx 2.5°$ at 88 K and $\approx 10°$ at 60 K; this slow variation appears to be consistent with the theoretical predicted weak temperature dependences.[10–12]

We stress that above $\varphi_T$, where according to the $m_{ab}$ measurements the vortex structure has become collinear, $\Delta m_c$ continues to fall over a significant further angular range (Fig. 8). This indicates that even in the collinear phase, the influence of TB pinning survives to larger angles. We see several possible explanations of this behavior: First, the minimum radius of curvature in the screening current distribution is the penetration depth λ, so that on small scales the shielding of the magnetic field becomes nonlocal. Consequently, around short (less than λ) trapped vortex segments, the direction of the internal field becomes collinear with the applied field. However, the vortex core remains in the kinked state, because its curvature is limited only by the much smaller coherence length $\xi$. A second possible explanation is the thermal excitation of vortex loops with a segment locked to the TB's; such loops provide an increased pinning force without generating any transverse magnetic moment.

We now turn to the relationship between $H_L$ and $\varphi_T$, for which theory suggests $H_L = H_{c1} \sin \varphi_T$.[11,12] Our experimental values, for example, at 60 K and 1 T, of $\varphi_T \approx 10°$ and $\mu_0 H_{L0} = 25$ mT, would require $\mu_0 H_{c1} \approx 150$ mT—several times higher than previously reported data which correspond to the range 30–50 mT (e.g., Ref. 20). There are two possibilities for this discrepancy: First, we might have incorrectly identified the angles corresponding to $\varphi_L$ and $\varphi_L$; however, the regular behavior of $H_{\max}(\varphi)$ [Fig. 6(a)] and the consistency between $\varphi_J$ and $\varphi_M$ (Fig. 8) support our analysis. An alternative is that the theories[10–12] oversimplify the interaction between vortices and TB's; for example, by neglecting the interaction with the image vortex. The exact calculation of the image interaction is nontrivial,[21] but as a rough estimate, the effect of a fully reflecting plane is to replace $H_{c1}$ with the thermodynamic critical field $H_c$ (as at a free surface); this gives much better agreement with our experimental values.

### F. Locking transition and the peak effect

Finally we discuss the dependence of the irreversible moment $\Delta m_c$ on magnetic field. In the twinned crystal OZ, $\Delta m_c(H)$ shows structure that, within a narrow angular range around the $c$ axis, is extremely sensitive to the field orientation (Fig. 9). In untwinned crystals, the response is essentially angle independent in this regime, as exemplified by the data for crystal MK in Fig. 8.

The twinned crystal data show a high-field peak that precedes a rapid fall in $\Delta m_c$; the magnitude of this peak $\Delta m_{\max}$ falls off quite rapidly with angle [Fig. 10(a)], but its position $H_{\max}$ changes only slowly [Fig. 10(b)]. Notice again that at angles above trapping angle ($\varphi_T \approx 2°$ at $T = 82$ K and $\mu_0 H = 1$ T), the continuing decrease in $\Delta m_c$ indicates the persistence of the effects of TB pinning well into the apparently collinear phase (at $T = 82$ K, up to $\varphi = 10°$–$15°$).

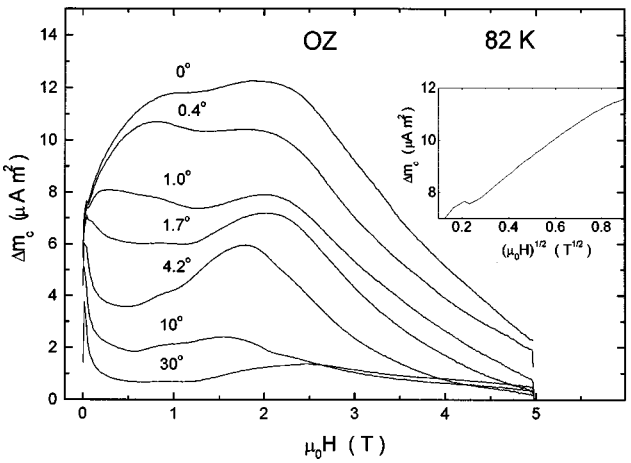


FIG. 9. Magnetic field dependences of the irreversible moment $\Delta m_c$ at 82 K of the twinned crystal OZ for a succession of angles between **H** and the TB plane; the fields are large compared with the penetration field of about 20 mT for $\varphi = 0$. Inset: $\Delta m_c$ plotted against $\mu_0 H^{1/2}$ for $\varphi = 0$.

In addition, when **H** is within a degree or so of the $c$ axis, a subsidiary maximum or shoulder is visible at lower fields (Fig. 9); its location shifts rapidly to lower fields as $\varphi$ increases [Fig. 10(b)].

Neither of these features is associated with vortex channeling,[7,8] because that phenomenon causes a *minimum* in $\Delta m_c$ when **H** is aligned precisely with the $c$ axis.

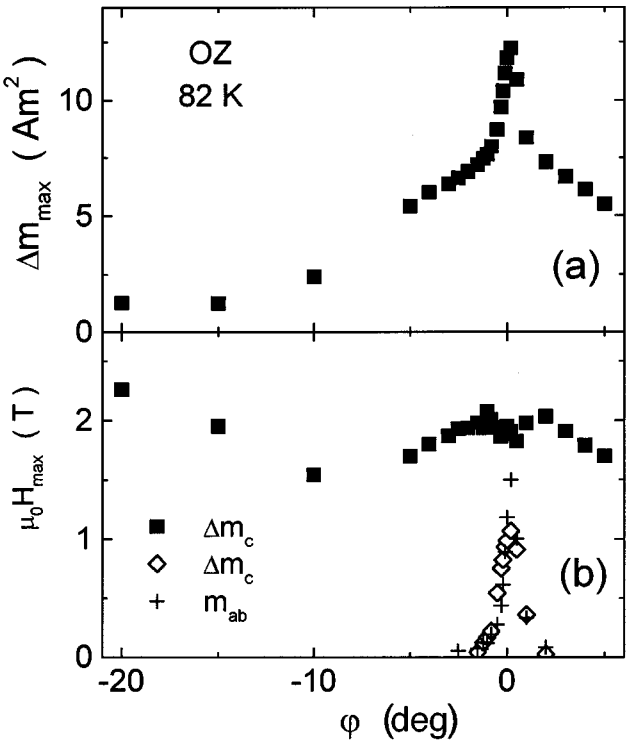


FIG. 10. Angular dependence of (a) the magnitude and (b) the position of the high-field peak of $\Delta m_c(H)$ (■) for crystal OZ at 82 K. (b) Shows also the positions of the subsidiary peak in $\Delta m_c(H)$ (◇) and the maxima of $m_{ab}(H)$ (+) at the same temperature; the latter is a signature of the collapse of the locked state.

We note that the position of subsidiary peak of $\Delta m_c$ coincides with the maximum of the transverse moment $m_{ab}$ [Fig. 10(b)]; as we discussed in Sec. III D, that maximum marks the boundary of the locked phase. We suggest therefore that the subsidiary peak in $\Delta m_c$ is another signature, albeit a weak one, of the locked phase boundary.

Near the $c$ axis and for fields below the subsidiary peak, and so within the locked phase, $\Delta m_c$ increases approximately as $H^{1/2}$ (Fig. 9, inset). There are two theories[21,22] that predict an increase of the pinning force parallel to the TB planes and with the critical current density, and so also $\Delta m_c$, increasing as $H^{1/2}$; both are related to vortex shear. A similar dependence of $\Delta m_{ab}$ was observed recently for **H** parallel to the $ab$ plane and simultaneously aligned closely to the TB planes.[23]

## IV. CONCLUSIONS

We have obtained clear experimental evidence of vortex locking phenomena in $YBa_2Cu_3O_7$ single crystals. The measurements show unambiguously that the direction of the vortices deviates from the applied field and is attracted to the twin boundary planes. The most decisive signature is the near-perfect and reversible shielding of the transverse field component, but associated features are visible too in the irreversible moment $\Delta m_c$ induced by screening currents that circulate within the $ab$ planes.

The transitions between the different vortex phases appear to be smeared rather than sharp, probably because of thermal activation and other factors. Even so, we are able to suggest criteria for identifying the locking and trapping angles for the vortex interaction with TB's; the dependences of these angles on field and temperature are similar to those predicted by theory, but their magnitude disagrees. Furthermore, within the apparently collinear phase, there are clear indications of the persistence of the influence of TB pinning. Our results indicate that the general approach to an understanding of the vortex interaction with TB's is correct, but that it is still in need of further development.

## ACKNOWLEDGMENTS

The authors are grateful to M. Klaser for the preparation of the detwinned MK and WZ crystals, and to V. M. Vinokur for useful discussions. This work was supported by NATO Linkage Grant No. HT931241, the UK Engineering and Physical Sciences Research Council, and the Russian Fund for Fundamental Research Grant No. 96-02-18376a.

[1] L. Ya Vinnikov *et al.*, Solid State Commun. **67**, 421 (1988); C. J. Dolan *et al.*, Phys. Rev. Lett. **62**, 827 (1989).
[2] C. A. Duran *et al.*, Nature (London) **357**, 474 (1992).
[3] V. K. Vlasko-Vlasov *et al.*, Phys. Rev. Lett. **72**, 3246 (1994); L. A. Dorosinskii *et al.*, Physica C **235-240**, 2727 (1994).
[4] G. W. Crabtree *et al.*, Phys. Rev. B **36**, 4021 (1987); L. J. Swartzendruber *et al.*, Phys. Rev. Lett. **64**, 483 (1990); J. Z. Liu *et al.*, *ibid.* **66**, 1354 (1991); U. Welp *et al.*, Appl. Phys. Lett. **57**, 84 (1990); D. L. Kaiser *et al.*, J. Appl. Phys. **70**, 5739 (1991); A. A. Zhukov *et al.*, Superconductivity (KIAE) **4**, 1268 (1991); A. A. Zhukov *et al.*, Phys. Rev. B **51**, 12 704 (1995).
[5] W. K. Kwok *et al.*, Phys. Rev. Lett. **64**, 966 (1990); B. Roas *et al.*, *ibid.* **64**, 479 (1990); G. W. Crabtree *et al.*, Physica C **185-189**, 282 (1991); S. Flesher *et al.*, Phys. Rev. B **47**, 14 448 (1993); J. N. Li *et al.*, *ibid.* **48**, 6612 (1993); V. F. Solovjov *et al.*, *ibid.* **50**, 13 274 (1994).
[6] W. M. Gyorgy *et al.*, Appl. Phys. Lett. **56**, 2465 (1990); B. Janossy *et al.*, Physica C **170**, 22 (1990); R. Hergt *et al.*, Phys. Status Solidi A **129**, 1 (1992).
[7] M. Oussena *et al.*, Phys. Rev. B **51**, 1389 (1995); Phys. Rev. Lett. **76**, 2559 (1996).
[8] A. A. Zhukov *et al.*, Phys. Rev. B **52**, R9871 (1995).
[9] H. Küpfer *et al.*, Phys. Rev. B **54**, 644 (1996).
[10] G. Blatter *et al.*, Phys. Rev. B **43**, 7826 (1991).
[11] G. Blatter *et al.*, Rev. Mod. Phys. **66**, 1125 (1994).
[12] E. B. Sonin, Phys. Rev. B **48**, 10 487 (1993).
[13] Th. Wolf *et al.*, J. Cryst. Growth **96**, 1010 (1989).
[14] D. Lacey *et al.*, Supercond. Sci. Technol. **8**, 568 (1995).
[15] F. Hellman *et al.*, Phys. Rev. Lett. **68**, 867 (1992).
[16] A. A. Zhukov *et al.* Phys. Rev. B **56**, 2809 (1997).
[17] B. Janossy *et al.*, Physica C **246**, 277 (1995); F. Steinmeyer *et al.*, Europhys. Lett. **24**, 459 (1994); V. Vulcanescu *et al.*, Phys. Rev. B **50**, 4139 (1994).
[18] A. A. Zhukov *et al.*, Physica C (to be published).
[19] L. Klein *et al.* Phys. Rev. B **49**, 4403 (1994).
[20] E. Z. Meilikhov and V. G. Shapiro, Superconductivity (KIAE) **4**, 1437 (1991).
[21] A. Gurevich and L. D. Cooley, Phys. Rev. B **50**, 13 563 (1994).
[22] K. I. Kugel *et al.*, Czech. J. Phys. **46**, 1025 (1996).
[23] L. M. Fisher *et al.* (unpublished).